Motor Control, 2007, **11**, 136-150

Pumping a Playground Swing

Auke A. Post, Gert de Groot, Andreas Daffertshofer, and Peter J. Beek

In mechanical studies of pumping a playground swing, two methods of energy insertion have been identified: parametric pumping and driven oscillation. While parametric pumping involves the systematic raising and lowering of the swinger's center of mass (CM) along the swing's radial axis (rope), driven oscillation may be conceived as rotation of the CM around a pivot point at a fixed distance to the point of suspension. We examined the relative contributions of those two methods of energy insertion by inviting 18 participants to pump a swing from standstill and by measuring and analyzing the swing-swinger system (defined by eight markers) in the sagittal plane. Overall, driven oscillation was found to play a major role and parametric pumping a subordinate role, although the relative contribution of driven oscillation decreased as swinging amplitude increased, whereas that of parametric pumping increased slightly. Principal component analysis revealed that the coordination pattern of the swing-swinger system was largely determined (up to 95%) by the swing's motion, while correlation analysis revealed that (within the remaining 5% of variance) trunk and leg rotations were strongly coupled.

Key Words: swinging, swing mechanics, parametric pumping, driven oscillation, coordinative structure, PCA

Swinging on a playground swing has been studied extensively as a biological example of the well-known physical pendulum (Burns, 1970; Case, 1996; Case & Swanson, 1990; Curry, 1976; Gore, 1970; McMullan, 1972; Simon & Riesz, 1979; Tea & Falk, 1968; Walker, 1989). The initiation of the swinging motion and the angular displacement of the swing are realized by the swinger pumping energy into the swing-swinger pendulum by means of bodily movements.

Two methods of energy insertion have been identified in mechanical analyses of this phenomenon. The first, called parametric pumping, consists of alternately raising and lowering the swinger's center of mass (CM) along the swing's radial axis (see Figure 1A). This method of energy insertion has been studied by modeling the swing-swinger system as a point mass at the end of a rope whose length is varied periodically, amounting to a parametric oscillation (Burns, 1970; Curry, 1976; Tea & Falk, 1968). If the sum of the external moments is small, the angular momentum is nearly constant: raising the CM yields a decrease in the moment of inertia I (with respect to the suspension point) and thus a proportional increase in

The authors are with the Research Institute MOVE, Faculty of Human Movement Sciences, VU University, Amsterdam, The Netherlands.

the angular velocity $\dot{\phi}$ and therefore the kinetic energy $E_{kin} = I\dot{\phi}^2/2$ of the swing. The largest energy gain is achieved when the swing moves through its lowest position: at this position the rise in CM and thus the increase in angular momentum is maximal. Assuming extensive movement of the swinger along the radial axis, several authors (e.g., Burns, 1970; Curry, 1976; Tea & Falk, 1968; Walker, 1989) have suggested that this method of energy insertion would be observed in a standing swinger.

The second method to pump energy into a swing, called "driven oscillation," is based on leaning back and forth during specific phases of the swing's motion (Gore, 1970; McMullan, 1972). The driving mechanism is an exchange between angular momentum due to rotation about the CM and angular momentum due to motion of CM about the suspension point (see Figure 1B).

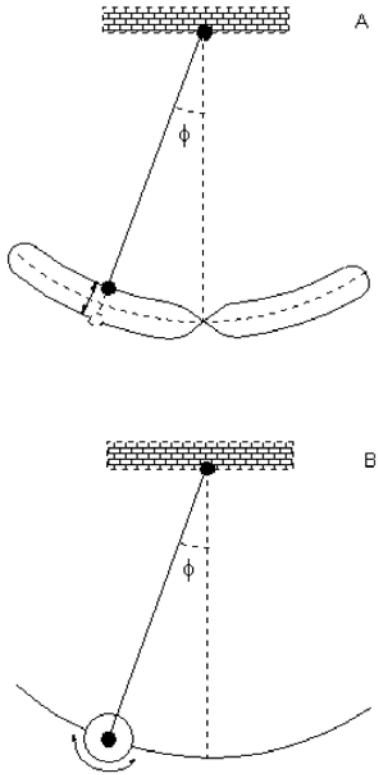

Figure 1—Schematic representation of the trajectory of the center of mass (CM) during parametric pumping (A) and during driven oscillation (B). In (A), the distance between the CM and the point of suspension varies. In (B), CM traverses a segment of a circle at a fixed distance to the point of suspension.

Energy insertion into the swing-swinger system has been examined in considerable analytical detail by Case (1996) and Case and Swanson (1990). Case (1996) introduced a rigid body with its CM rotating with respect to a pivot point at the lower end of a suspension rope. In the resonant case, that is, if the swinger pumps at the swing's natural frequency ω, the rotation angle ϕ obeys the following equation of motion:

$$\ddot{\phi} + \omega^2 \phi = F \cos \omega t + A\phi \cos 2\omega t + B\dot{\phi} \sin 2\omega t + C\ddot{\phi} \cos 2\omega t \qquad (1)$$

This equation represents a harmonic oscillator that is driven by an external force which varies harmonically in time, as expressed by the driving term $F\cos\omega t$, and parametric terms $A\ldots$, $B\ldots$, and $C\ldots$, which modify the oscillator's parameters at higher harmonics. If ϕ is small, then these parametric terms vanish, resulting in driven oscillation. Conversely, if ϕ grows, the parametric terms dominate the equation resulting in a form of oscillation in which parametric pumping prevails. Formal analyses of the equation of motion suggested that an actual swinger will hardly pump parametrically, but will mainly pump energy into the swing in the driven oscillator mode (Case, 1996; Case & Swanson, 1990). These predictions were based on estimated numerical values for the parameters for an adult swinger.

In spite of these predictions, however, actual swinging behavior and the relative contributions of parametric pumping and driven oscillation have not been investigated empirically to date. For the present experimental study, we chose to perform the analysis in a local (moving) 2D Cartesian coordinate system with one coordinate axis fixed to the swing's rope (radial motion) and the other one orthogonal to it (tangential motion). As explained in the preceding section, the radial motion of the CM can be associated with parametric pumping and its tangential motion with driven oscillation. For effective swinging these two different regimes are characterized further by distinct phasing relations with respect to the swing's rotation. The driven oscillation regime requires that the CM is displaced mainly at the turning points, but remains steady when the swing passes through its lowest point. The driven oscillation is approximately 90° or 270° shifted in phase with respect to the swing's motion, which should be visible in the phasing of the tangential movements of the CM. In contrast, the parametric pumping regime requires that the CM be displaced mainly when the swing passes through its lowest point during the fore (or back) swing, but remains steady at the extremes. Hence, parametric pumping is approximately 0° or 180° shifted in phase with respect to the swing's motion, which should be visible in the phasing of the radial movements of the CM. These expectations can be tested by calculating the cross-correlation function between each CM component and the swing angle to determine the time lag, and subsequently, by using the basic frequency of swinging, the relative phase at which phase locking occurred. After all, under both regimes the movement of the swinger should vary harmonically with the frequency of swinging.

The identified methods of energy insertion are brought about by coordinated actions of a multisegmental movement system, the human body. The pattern of intersegmental coordination observed in a human swinger on a playground swing may be viewed as an example of a coordinative structure or synergy (Kugler, Kelso, & Turvey, 1980). A coordinative structure is a temporal arrangement of body components in two regards: first, it exists for a limited time only, namely as long as the activity persists; second, it specifies the temporal relations between these

components in terms of their (relative) phasing. Coordinative structures have often been examined by pair-wise comparisons of the time series representing individual limb movements (i.e., cross-correlations or relative phase analyses). However, this requires an a priori decision on the part of the experimenters about which time series are relevant and which are not. A method that avoids such an arbitrary step is principal component analysis (PCA). The relevance of PCA for the analysis of human movement is exemplified by its successful application in studies examining standing (Alexandrov, Frolov, & Massion, 1998; Vernazza-Martin, Martin, & Massion, 1999), walking (Mah, Hulliger, Lee, & O'Callaghan, 1994), reaching (Jaric, Ferreira, Tortoza, Marconi, & Almeida, 1999; Pigeon, Yahia, Mitnitski, & Feldman, 2000), pedalo riding (Haken, 1996), and juggling (Post, Daffertshofer, & Beek, 2000)—see Daffertshofer, Lamoth, Meijer, and Beek (2004) for a tutorial. As analysis literally means "breaking down into constituent elementary parts," principal components or modes can be conceived as these "independent" parts, which—by PCA's very definition—do not covary with each other. Interestingly, principal modes may be associated with the basic synergies or coordinative structures (Turvey, 1990) that constrain the movement system into a functional unit with a limited number of degrees of freedom (see also, Post, Peper, & Beek, 2000; Schöner, 1995; Scholz, Danion, Latash, & Schöner, 2002). These dimensions capture the task and the participant's behavior in increasing detail; in other words, the largest mode is the most important but crude descriptor of the behavior, which in swinging takes the form of a phase coupled set of body segments oscillating at a shared frequency in a specific direction. The subsequent modes describe the movements in a different direction, possibly with different phase relations and at a different frequency. Once the most important components of the swinging movement have been identified by PCA, further analyses of the coordination of interest can be performed using cross-correlation functions to determine the relative phase at which an optimal coupling occurs.

In sum, we analyzed the pumping of a playground swing from standstill in two steps. First, we examined the relative contributions of the two proposed models of energy insertion by comparing tangential and radial components of the CM motion, representing driven and parametric oscillations, respectively. Next, we analyzed the principal components of intersegmental coordination within the swing-swinger system to gain insight into the coordinative structure via which energy insertion was achieved. In both steps, we calculated cross-correlation functions between selected variables to determine the time lag, and subsequently the relative phase, at which the variables in question were coupled most strongly.

Methods

Eighteen individuals (mean age 29.4 years, *SD* 6.6 years) participated in the experiment. Prior to this, participants were informed about the purpose and procedures of the experiment and signed an informed consent statement. Height and weight of the participants were measured in order to estimate the centers of mass of all body segments using anatomical regression equations (Plagenhoef et al., 1983).

Participants were asked to start the seated swinging motion from rest and to gradually increase its amplitude without making contact with the ground. They were instructed to perform the swinging movements as smoothly and as regularly

as possible. They were further instructed to actively engage in each swing cycle. Participants were given three 10 s practice trials, after which the experiment proper was started. The experiment consisted of five trials lasting 30 s each. In a separate trial, during which the participants were instructed to sit still on the swing, the location of the CM at rest was determined.

Data Processing

Participants swung on a playground swing (RESPO model 8000). The distance between the floor and the center of the swing's rotation axis was 2.58 m, the length of the suspension chains was 1.75 m, and the dimensions of the seat were 0.44 m (width) and 0.22 m (depth).

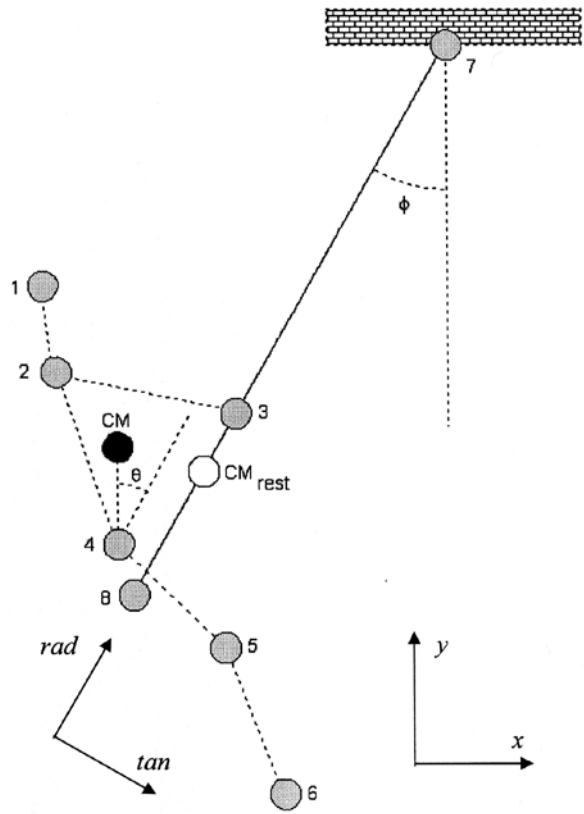

Figure 2—Schematic side view of landmarks on a seated swinger (numbers 1 through 6) and on the swing (numbers 7 and 8) defining the angles ϕ and θ. CM: actual position of center of mass; CM_{rest}: position of CM when subject and swing are in rest. The fixed x-y coordinate system and the moving radial and tangential system are shown as well.

Swinging patterns of the participants were recorded with an active marker system (Northern Digital Optotrak system 3020), consisting of a single control unit operating two measurement systems each housing three position sensors. Infrared light emitting diodes (LEDs) were placed on specific body landmarks: head just above the ear (1), shoulder (2), distal part of the third metacarpal (3), hip at the level of the trochanter major (4), lateral epicondyle of the femur (5), and lateral malleolus (6)—see Figure 2. Two additional markers were attached to the swing's seat and rotation point, markers (8) and (7), respectively, which are also indicated in Figure 2. Data were digitized at a sampling rate of 150 Hz. Missing samples in the digital data due to occlusion by the swing's frame were linearly interpolated. The data were subsequently filtered with a bi-directional fourth-order Butterworth low-pass filter (cutoff frequency was 10 Hz for the horizontal component (x) and 5 Hz for the vertical component (y) of the position data because the swing frequency in the vertical direction is twice the frequency in the horizontal direction).

Data Analysis

The (x, y) position of the whole body's CM was calculated from the position and orientation of body segments and swing as given by the recorded marker coordinates. Next, the (x, y) coordinates of CM were transformed to the aforementioned ϕ-rotated moving coordinate system (rad, tan), in which the radial direction pointed from marker (8) to (7) and the tangential direction was perpendicular to that direction; the origin was chosen at $\mathrm{CM}_{\mathrm{rest}}$ (cf. Figure 2). In general, the swing is driven by the swinger forcing the angle θ to vary (the hip being the pivot). We analyzed this angle's degree of harmonicity to compare performance with previous studies (e.g., Simon & Riesz, 1979). To this end, the time series of θ were analyzed in the spectral domain (Welch's periodogram method with non-overlapping Hamming windows). The dominant frequency ω_0 was established and the power in a bandwidth of ± 10% around this frequency was integrated, as was done for the equivalent bands of the nine subsequent higher harmonics (ω_1, ω_2, …, ω_9). The sum of the spectral power of those harmonics was normalized to an integral of unity (see, e.g., Peper et al. 1995) yielding the following measure of harmonicity H

$$H = 1 - \frac{\sum_{i=1}^{9} \int_{0.9\omega_i}^{1.1\omega_i} P(\omega)\, d\omega}{\int_{0.9\omega_0}^{1.1\omega_0} P(\omega)\, d\omega} \tag{2}$$

An H-value of 1 implies a perfectly harmonic sinusoid (i.e., all power is contained at the dominant frequency) and the smaller H, the larger the presence of higher harmonics relative to the dominant frequency. Note that, in general, H can become negative but this requires rather large amounts of spectral power at the higher harmonics, a scenario that is unlikely in the present case in which the overall motion is more or less sinusoidal (i.e., the power spectrum quickly decays to zero).

Time series of the radial displacement CM_{rad} and the tangential displacement CM_{tan} were obtained. Peaks of these time series were detected in order to calculate amplitudes A_j, i.e. $A_j = \left(\max_j - \min_j\right)/2$ per each cycle j. The first derivative (or

difference) of the amplitudes was calculated as $V_j = A_{j+1} - A_j$ per cycle *j* for a first-order assessment of the energy dynamics. Both amplitudes and derivatives were averaged over cycles yielding the corresponding means denoted as $\overline{A}$ and $\overline{V} = \overline{dA/dt}$. Further, these mean values were averaged over five identical trials per participant and used to test which energy insertion method was used (i.e., $\overline{A}_{rad} \neq 0, \overline{A}_{tan} = 0$) for parametric pumping or $\overline{A}_{rad} = 0, \overline{A}_{tan} \neq 0$ for driven oscillation). Subsequently, we evaluated whether this initial situation was maintained throughout the trial (i.e., $\overline{V}_{rad} = \overline{V}_{tan} = 0$) or whether both methods were (alternatively) used with one being more important than the other (i.e., $\overline{A}_{rad} > \overline{A}_{tan}$ or $\overline{A}_{rad} < \overline{A}_{tan}$). Finally, we examined whether a change occurred in the relative contributions of these methods of energy insertion (i.e., $\overline{V}_{rad} > 0, \overline{V}_{tan} < 0$ or $\overline{V}_{rad} < 0, \overline{V}_{tan} > 0$).

For the PCA, the time series of the (*x*, *y*) coordinates of all eight markers (rather than the radial and tangential components) were used as input. In view of holonomic constraints (i.e., fixed segment length reducing a pendulum to a two-dimensional motion) PCA was expected to yield two modes with a phase shift of 90º per oscillation (see Daffertshofer et al., 2004). For each trial the following procedure was applied: eigenvalues (variances) and eigenvectors (coefficients) of the 16 × 16 covariance matrix were determined and the original dataset was projected onto the eigenvectors yielding 16 time series $\xi_k(t)$ (scores); modes were grouped in pairs (i.e., two dimensions) because these pairs matched the (two-dimensional) planar swing movement (with geometrical constraints, e.g., fixed limb length); and, finally, eigenvalues were *z*-transformed before averaging over identical trials per participant (the reported averaged values were inversely transformed).

Cross-correlation functions were calculated for three pairs of time series to establish their degree of coupling. The pairs of time series in question were (a) CM_{tan} and the swing's oscillation ϕ, (b) CM_{rad} and ϕ, and (c) the rotation angle of the trunk (α) and the rotation angle of the lower leg (β). Segmental angular rotations were measured with respect to the vertical. The pairs of time series were correlated with a variable time delay τ to assess the coupling between both time series, which yielded the cross-correlation ρ as a function of τ (after normalization ρ became bounded between -1 and 1). Subsequently, the value of τ was determined at which the two time series were optimally correlated, as indicated by the highest value of ρ. Cross-correlations at this optimal time lag were used as dependent measures. Time lags were used to calculate the phase difference ψ (in degrees) between the swing's oscillation and the variable of interest, using the previously calculated ψ_0. All ρ and τ values were subsequently averaged over five identical trials per participant (ρ values were *z*-transformed to ensure normality). The averaged values of (a) and (b) were used to evaluate whether the coupling between the tangential component and the swing was as strong as the coupling between the radial component and the swing, and whether there existed a difference in phasing between the tangential and the radial component with respect to the swing. Specifically, the obtained τ values could be tested against mathematically derived values (Case, 1996) to evaluate whether the phase difference between tangential movement and swing motion was 90°, and whether the phase difference between radial movement and swing motion was 180°.

Statistics

Variables were analyzed with one-sample *t*-tests: $\overline{A}_{rad}$, $\overline{A}_{tan}$, $\overline{V}_{rad}$, $\overline{V}_{tan}$ against 0, τ (CM_{tan},ϕ) against 90° and τ (CM_{rad},ϕ) against 180°); or with paired-samples *t*-tests: $\overline{A}_{rad}$ versus $\overline{A}_{tan}$, $\overline{V}_{rad}$ versus $\overline{V}_{tan}$, and $\rho(CM_{tan},\phi)$ versus $\rho(CM_{rad},\phi)$; we used a significance level of $\alpha = .05$.

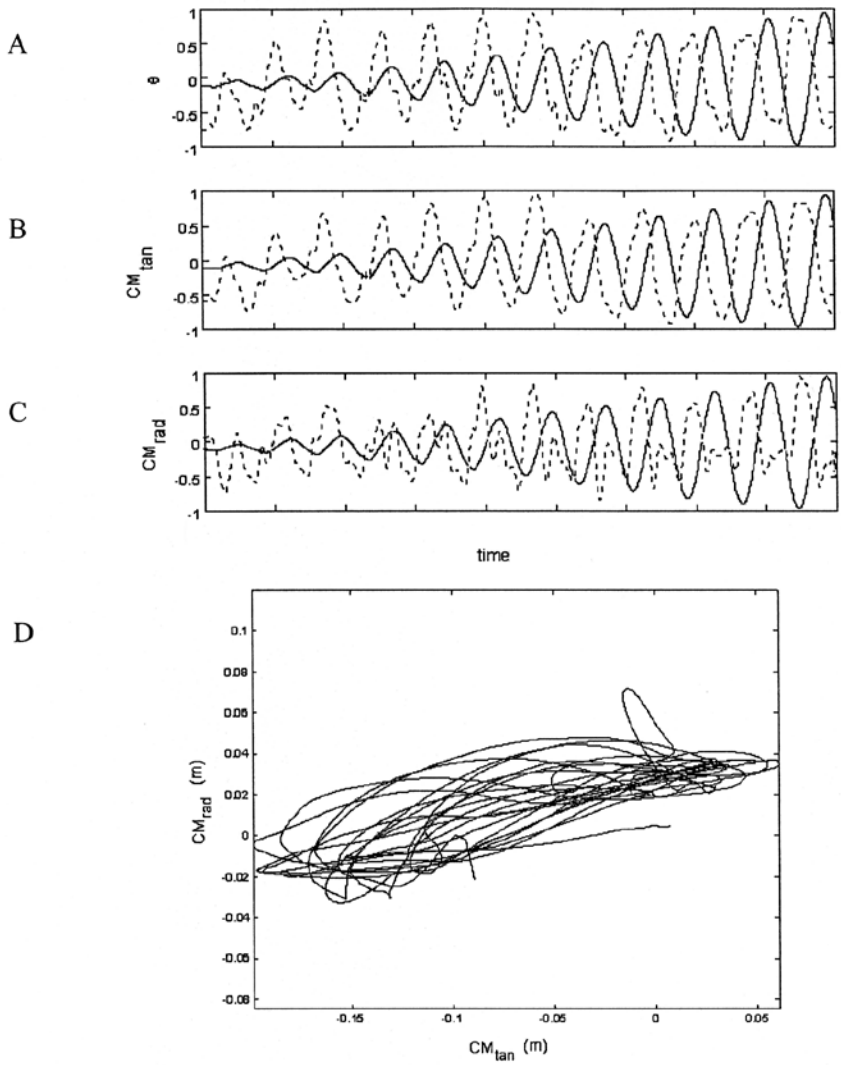

Figure 3—Normalized time series of ϕ (solid line) and θ (dashed line) (panel A), CM_{tan} (panel B) and CM_{rad} (panel C); positive values: right (CM_{rad}), down (CM_{tan}), counterclockwise (ϕ) or clockwise (θ). Panel D: Example of the CM trajectory in radial and tangential components. Note the difference in scale factor used on the abscissa and ordinate.

Results

Relative Contribution of Driven Oscillation and Parametric Pumping

All participants were able to pump the swing close to the indicated maximal amplitude: the average value of ϕ_{max} was 65.2° (*SD* 4.2°). The preferred frequency was nearly the same for all participants with an average of 0.384 Hz (*SD* 0.004 Hz). The swing is driven by variation of the angle θ. A typical example of the time series of ϕ and θ is given in Figure 3A. For all trials, the mean value of the harmonicity H was .97, i.e., fairly close to 1 implying an almost purely sinusoidal motion. This finding supports a harmonic driving force like the F…-term used in Equation 1. Figure 3 also shows a typical example of the CM time series and trajectory relative to its rest position during a trial. Essentially the same CM motion was observed in all trials. Obviously, CM trajectories were not symmetrical. The CM hardly passed the swing rope, which means that the major part of the energy insertion was achieved by leaning backward.

The averaged values of the dependent variables are listed in Table 1. The mean values of $\overline{A}_{rad}$, $\overline{A}_{tan}$ and $\overline{V}_{tan}$ differed significantly from zero ($t_{17} = 3.30, -18.26$, and -3.42, respectively, $p < .05$), indicating marked contributions of both methods of energy insertion. Only $\overline{V}_{rad}$ did not differ significantly from zero indicating that the radial amplitude remained statistically constant in the course of a trial. To evaluate the relative importance of both methods of energy insertion we tested $\overline{A}_{rad}$ against $\overline{A}_{tan}$ and found that $\overline{A}_{rad} < \overline{A}_{tan}$ ($t = -19.18, p < .05$), indicating that the contribution in radial direction was not as great as that in tangential direction. We further tested $\overline{V}_{rad}$ against $\overline{V}_{tan}$ and found that $|\overline{V}_{tan}|$ was much larger than $|\overline{V}_{rad}|$ ($t = 4.22, p < .05$) and that $\overline{V}_{rad}$ and $\overline{V}_{tan}$ differed in sign. These results indicate that $\overline{A}_{tan}$ decreased in the course of a trial, while $\overline{A}_{rad}$ increased, albeit to a much lesser extent. Taken together, these results revealed that the tangential movements prevailed during the whole trial, indicating that the swing-swinger system predominantly behaved as a driven oscillation, with a subordinate role for parametric pumping. However, in

Table 1 Mean Values of the Dependent Variables (Averaged Over Identical Trials and Subjects): Amplitudes A in M, Velocities V in M/S, Phase Difference ψ in Degrees and PCA Eigenvalues in Percent

variable	mean	variable	mean	variable	mean
$\overline{A}_{rad}$	0.0164*	$\rho(CM_{rad},\phi)$	.68	PCA12	95.18
$\overline{A}_{tan}$	–0.0836*	$\psi(CM_{rad},\phi)$	132.9	PCA34**	96.91
$\overline{V}_{rad}$	0.0005	$\rho(CM_{tan},\phi)$	.74	PCA56**	2.34
$\overline{V}_{tan}$	–0.0026*	$\psi(CM_{tan},\phi)$	104.4	$\rho(\alpha,\beta)$	0.96

* significantly different from zero

** after removal of the first two modes and rescaling the residual to 100%

the course of a trial, that is, as the amplitude of swinging increased, the tangential amplitude decreased and the radial amplitude tended to increase, indicating a gradual shift in emphasis from driven oscillation to parametric pumping, as predicted (Case, 1996; Case & Swanson, 1990).

The cross-correlation functions between CM_{tan} and ϕ and between CM_{rad} and ϕ revealed that the tangential as well as the radial component of CM were coupled to the swing's motion ($\rho = .74$ and .68, respectively; see Table 1), indicating again that both driven oscillation and paramertric pumping were operative. However, optimal coupling occurred at an averaged phase lead of 104.4° for CM_{tan} and at an averaged phase lead of 132.9° for CM_{rad}, both of which differed significantly from the predicted values for driven oscillation ($\psi(CM_{tan},\phi) \neq 90°$, $t = 2.95$, $p < .05$) and 180° for parametric pumping (($\psi(CM_{rad},\phi) \neq 180°$, $t = -7.57$, $p < .05$).

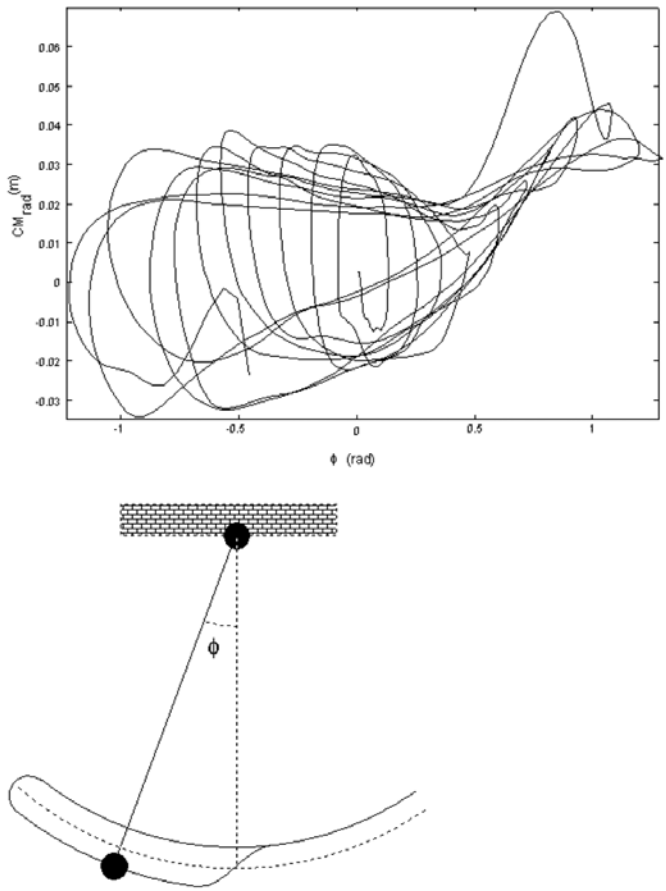

Figure 4—A: Representative example of the radial component of the center mass (CM_{rad}) against the swing's angle with the gravitational vertical (ϕ). B: Schematic trajectory in *x*-*y* plane of CM during swinging.

To provide an impression of the behavior of CM, Figure 4A depicts the radial movement of CM as function of ϕ from the time series shown in Figure 3C. The swinger's CM was lowered by "falling back" at the rear end of the swing movement and was gradually raised while swinging forward. This rise contributed to the increase of angular velocity, partially resembling the path followed during parametric pumping (cf. Figure 4B). The pumping primarily took place in the very last part of the back-swing and the first part of the fore-swing, thereby underscoring the fact that effective swinging was based on a tight phase locking between the swing's rotation and the activity of the swinger as reflected in CM_{tan} and CM_{rad}. The finding that a similar pumping mechanism was not observed in the back-swing can be understood via anatomical constraints that precluded leaning forward during the back-swing (together with the risk of falling forward). Note that this observed single oscillation of the CM in radial direction per half swing cycle is, in terms of frequency, consistent with the double oscillation per swing cycle involved in the parametric terms in Equation 1.

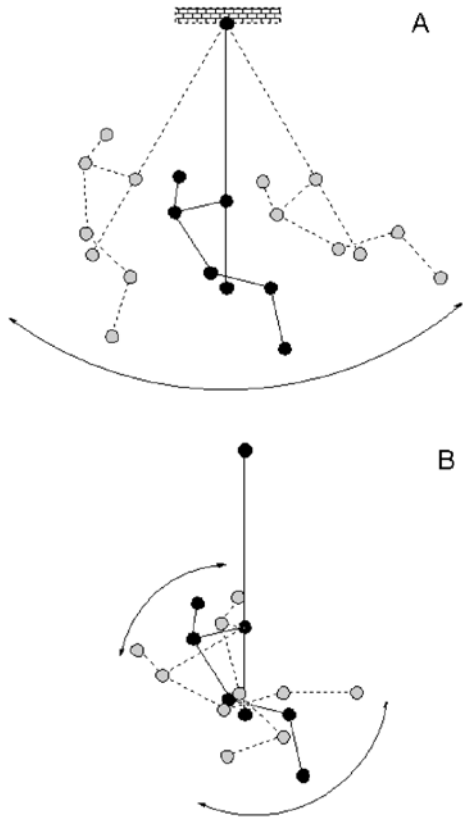

Figure 5—Stick diagrams of the projections of the most relevant PCA modes. A: PCA12 (passive whole body movement with swing, α and β constant), B: PCA34 (coordinated movements of trunk and lower leg with respect to swing rope).

Analysis of the Coordination Pattern of Swinging

Also the results of the PCA analysis are summarized in Table 1, collapsed over identical trials and participants. A small number of modes accounted for nearly all the variance in the swing-swinger system: of the 16 available modes (eight markers in two directions), the first four readily accounted for 99% of the total variance. Since all markers cover a comparable range of amplitude values, this quick drop of eigenvalues implies a rather stringent coordination and, hence, a dramatic reduction of the dimensionality of the system: for an adequate description of this 16-dimensional system only 4 dimensions suffice. After projecting the original data on the coordinate system spanned by the principal axes, it appeared that the first two modes (PCA12) coincided with the passive large swing movement (i.e., the swing oscillating in *x*- and *y*-direction; see Figure 5A). Interestingly, these two modes already accounted for approximately 95% of the total variance, that is, the movements of the swinger were largely subordinate to the mechanical motion of the swing. Removing the first two modes and rescaling the sum of all the remaining modes to 100% allowed us to examine these remaining modes more closely in a "decompressed" form. As became apparent from the projections, the remaining modes represented the movements of the swinger with respect to the swing. The first two modes of this reduced set (PCA34) could be associated with synchronous isodirectional trunk-leg rotations (see Figure 5B) and accounted for as much as 97% of the swinger's activity. The subsequent two modes (PCA56) indicated additional movements of the swinger (either along the rope of the swing or trunk-leg rotations with a phasing relation opposite to that of PCA34) representing an additional 2.5% of the activity. The sum of all remaining modes (7 to 16) was even after rescaling negligibly small (less than 1% of the total variance).

In view of those PCA results, the degree of trunk-leg coupling was examined further by calculating the cross-correlation function between the trunk angle α and the lower leg angle β (see Figure 6). Cross-correlations ρ are presented in Table 1 collapsed over identical trials but as function of trunk and lower leg angles, i.e., $\rho = \rho(\alpha,\beta)$. The high mean value ($\rho = .96$) indicates that α and β were strongly coupled. The angular rotation of the trunk somewhat lagged behind the angular rotation of the lower leg (the average value of ψ was 16.0°), but this could simply be the result of a difference in inertia. All in all, it appears that trunk and legs were not controlled independently, but formed an integral part of the coordinative structure for swinging.

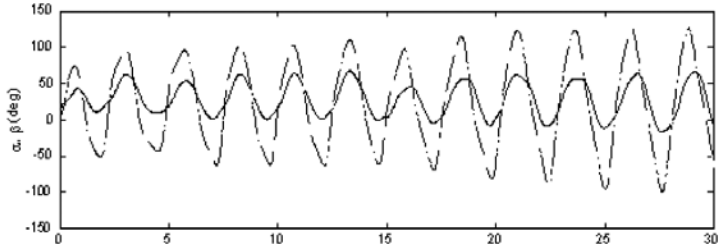

Figure 6—Trunk angle α (solid) and lower leg angle β (dashed) as functions of time.

General Discussion

The goal of the present study was to determine the extent to which the two methods of energy insertion identified in the physics literature, i.e., driven oscillation and parametric pumping, are involved in pumping a playground swing from standstill and to examine the corresponding coordinative structure of swinging. To this end, we conducted an experiment comparing real-life results with predictions derived from mechanical models. The results with regard to the two methods of energy insertion were largely in agreement with the main thrust of the mechanical analyses performed by Case (Case, 1996; Case & Swanson, 1990). As predicted for pumping a swing in a seated position, driven oscillation (as indexed by CM_{tan}) was found to play a major role and parametric pumping (as indexed by CM_{rad}) a subordinate role, although the relative contribution of driven oscillation decreased as swinging amplitude increased, whereas that of parametric pumping increased slightly. That both methods of energy insertion were operative was also evident from the fact that both CM_{tan} and CM_{rad} were phase coupled to the swing angle, albeit not at the predicted values of 90° and 180°, respectively. Instead, both components reached their maximal value while the swing moved from its rear turning point towards its lowest point (at phase leads of 104° and 133°, respectively).

The analysis of the coordinative structure of swinging using PCA revealed that the swinging motion is severely constrained by the mechanical properties of the swing-swinger system: 95% of the total variance could be attributed to the passive motion of the swing, implying that a mere 5% of the total variance was associated with active movements of the swinger. A "zoomed-in" PCA on this portion of the variance revealed that that the intersegmental coordination of the swinger mainly consisted of trunk-leg coordination. Further (correlation and relative phase) analyses of this coordination revealed that the rotations of trunk and lower legs were closely coupled with the lower legs leading the trunk by 16° while rotating over a much larger range of angles (cf. Figure 6). During this rotation, the knees were stretched leading to a CM change in tangential direction (i.e., the CM was slightly brought forward) and in radial direction (i.e., the CM was slightly lifted up). This displacement of the CM was partially countered by the onset of trunk rotation, which, in its first stage, was predominantly in tangential direction (i.e., the CM was slightly brought backward). Thus, the resulting CM movement was first in radial direction, and then quickly followed by movement in tangential direction. The fact that trunk and lower leg rotations cancelled each other out in the tangential direction for a brief moment may also explain the observed phase difference between tangential and radial movement on the one hand (29°), and between trunk and lower legs rotation on the other hand (16°).

In sum, it can be concluded that while the discussed mechanical models approximate the mechanics of playground swinging to a satisfactory degree, measurements and analyses of real-life swinging are indispensable for capturing essential details of task performance. As expected on theoretical grounds, humans predominantly employ the method of driven oscillation to pump a playground swing from standstill with a subordinate role for parametric pumping, which increases in significance with the amplitude of swinging. However, the complex, multisegmental movements performed by humans are such that CM and swing are phase locked at other than mathematically predicted values, and are characterized by a strong coupling between rotations of the trunk and the lower legs.

Acknowledgments

The authors wish to thank Bert Coolen and Bert Clairbois for their technical assistance. RESPO Company (Vroomshoop, the Netherlands) is gratefully acknowledged for the donation of the playground swing.

References

Alexandrov, A., Frolov, A., & Massion, J. (1998). Axial synergies during human upper trunk bending. *Experimental Brain Research*, **118**, 210-220.

Burns, J.A. (1970). More on pumping a swing. *American Journal of Physics*, **38**, 920-922.

Case, W.B. (1996). The pumping of a swing from the standing position. *American Journal of Physics*, **64**, 215-220.

Case, W.B., & Swanson, M.A. (1990). The pumping of a swing from the seated position. *American Journal of Physics*, **58**, 463-467.

Curry, S.M. (1976). How children swing. *American Journal of Physics*, **44**, 924-926.

Daffertshofer, A., Lamoth, C.J., Meijer, O.G., & Beek, P.J. (2004). PCA in studying coordination and variability: a tutorial. *Clinical Biomechanics*, **19**, 415-428.

Gore, B.F. (1970). The child's swing. *American Journal of Physics*, **38**, 378-379.

Haken, H. (1996). *Principles of brain functioning: A synergetic approach to brain activity, behavior and cognition*. Berlin: Springer Verlag.

Jaric, S., Ferreira, S.M.S., Tortoza, C., Marconi, N.F., & Almeida, G.L. (1999). Effects of displacement and trajectory length on the variability pattern of reaching movements. *Journal of Motor Behavior*, **31**, 303-308.

Kugler, P.N., Kelso, J.A.S., & Turvey, M.T. (1980). On the concept of coordinative structures as dissipative structures: I. Theoretical lines of convergence. In G.E. Stelmach & J. Requin (Eds.), *Tutorials in motor behavior* (pp. 3-47). Amsterdam: North-Holland.

Mah, C.D., Hulliger, M., Lee, R.G., & O'Callaghan, I.S. (1994). Quantitative analysis of human movement synergies: Constructive pattern analysis for gait. *Journal of Motor Behavior*, **26**, 83-102.

McMullan, J.T. (1972). On initiating motion in a swing. *American Journal of Physics*, **40**, 764-766.

Peper, C.E., Beek, P.J., & van Wieringen, P.C.W. (1995). Coupling strength in tapping a 2:3 polyrhythm. *Human Movement Science*, **14**, 217-245.

Pigeon, P., Yahia, L., Mitnitski, A.B., & Feldman, A.G. (2000). Superposition of independent units of coordination during pointing movements involving the trunk with and without visual feedback. *Experimental Brain Research*, **131**, 336-349.

Plagenhoef, S., Evans, G.E., & Abdelnour, T. (1983). Anatomical data for analyzing human motion. *Research Quarterly for Exercise and Sport*, **54**, 169-178.

Post, A.A., Daffertshofer, A., & Beek, P.J. (2000). Principal component analysis in three-ball cascade juggling. *Biological Cybernetics*, **82**, 143-152.

Post, A.A., Peper, C.E., & Beek, P.J. (2000). Relative phase dynamics in perturbed interlimb coordination: The effects of frequency and amplitude. *Biological Cybernetics*, **83**, 529-542.

Schöner, G. (1995). Recent developments and problems in human movement science and their conceptual implications. *Ecological Psychology*, **7**, 291-314.

Scholz, J.P, Danion, F., Latash, M.L., & Schöner, G. (2002). Understanding finger coordination through analysis of the structure of force variability. *Biological Cybernetics*, **86**, 29-39.

Simon, R., & Riesz, R.P. (1979). Large amplitude simple pendulum: A Fourier analysis. *American Journal of Physics*, **47**, 898-899.

Tea, P.L., & Falk, H. (1968). Pumping on a swing. *American Journal of Physics*, **36**, 1165-1166.

Turvey, M.T. (1990). Coordination. *American Psychologist*, **45**, 938-953.

Vernazza-Martin, S., Martin, N., & Massion, J. (1999). Kinematic synergies and equilibrium control during trunk movement under loaded and unloaded conditions. *Experimental Brain Research*, **128**, 517-526.

Walker, J. (1989). How to get the playground swing going: A first lesson in the mechanics of rotation. *Scientific American*, **260**, 86-89.